

Control of Saharan mineral dust transport to Barbados in winter by the Intertropical Convergence Zone over West Africa

O. M. Doherty,¹ N. Riemer,² and S. Hameed¹

Received 9 March 2012; revised 30 August 2012; accepted 30 August 2012; published 12 October 2012.

[1] The reasons for the inter-annual variability of dust transport from the Sahara across the Atlantic are not well-understood. Here we address this issue by defining three new climate indices that capture the position and intensity of the zone of near-surface convergence over West Africa, a part of the global Intertropical Convergence Zone (ITCZ). We then relate these indices to a 38-year record of mineral dust concentrations at Barbados focusing on the winter season. The results show that the latitudinal displacement of the ITCZ over West Africa and the dust load in Barbados are statistically significantly correlated with a correlation coefficient of $r = -0.69$. A southward movement of the ITCZ corresponds to an increased dust load at Barbados. This correlation represents an improvement upon previous results, which focused on traditional teleconnection indices such as the North Atlantic Oscillation or the El-Niño-Southern Oscillation. From analyzing composites of wind and precipitation we conclude that for the winter season, the inter-annual variability of the Barbados dust load is related to changes in near-surface northeasterly winds in semi-arid regions in North Africa coincident with the movement of the ITCZ. Changes in precipitation appear to only play a minor role.

Citation: Doherty, O. M., N. Riemer, and S. Hameed (2012), Control of Saharan mineral dust transport to Barbados in winter by the Intertropical Convergence Zone over West Africa, *J. Geophys. Res.*, 117, D19117, doi:10.1029/2012JD017767.

1. Introduction

[2] The largest source of mineral dust globally is the Saharan desert [Prospero *et al.*, 2002; Washington *et al.*, 2003]. Dust from this region is transported long distances over the North Atlantic Ocean [Darwin, 1846; Prospero *et al.*, 1970] and plays an important role in the climate system [Arimoto, 2001]. It exerts a direct radiative forcing on climate as it interacts with solar and longwave radiation [Sokolik and Toon, 1996; Tegen *et al.*, 1996]. Moreover, dust particles play an important role for various aspects of the microphysics of both mixed-phase clouds [DeMott *et al.*, 2003] and warm clouds [Levin *et al.*, 2005] and hence are an important contributor to the aerosol indirect effect. Saharan dust has been linked with the frequency and intensity of Atlantic hurricanes [Dunion and Velden, 2004; Evan *et al.*, 2006a; W. K. M. Lau and K.-M. Kim, 2007; K. M. Lau and K. M. Kim, 2007] and has been found to fertilize ocean waters with iron and other micronutrients [Jickells, 1999; Baker *et al.*, 2006], to promote algal blooms [Walsh and Steidinger, 2001], and to provide phosphate and potassium

to the Amazon Basin [Swap *et al.*, 1992]. The long-range transport of mineral dust from the Sahara across the Atlantic is significant enough to be responsible for the formation of the soils of many Caribbean islands and the Amazon Basin [Herwitz *et al.*, 1996; Muhs *et al.*, 2007].

[3] This long-range transport of mineral dust is subject to considerable inter-annual and intra-annual variability due to a number of physical factors. Winds over the Sahara and Sahel control emissions of mineral dust [Washington *et al.*, 2003; Washington and Todd, 2005], and winds downstream of the emission region affect subsequent transport [Chiapello *et al.*, 1995; Riemer *et al.*, 2006; Doherty *et al.*, 2008]. Precipitation and vegetation in the Sahel has been suggested as a key factor in dust emission processes [Evan *et al.*, 2006b]. Precipitation over the source region can modulate dust emission, and precipitation over the transport region can remove dust from the atmosphere [Tegen and Fung, 1994; Zender *et al.*, 2003].

[4] The variability of mineral dust transport from Africa across the Atlantic is documented in the long-term mineral dust record measured at Barbados. Dust concentrations have been measured and published at this locations from 1965 through 2003 and have been studied extensively by the community [Rydell and Prospero, 1972; Prospero and Nees, 1977; Glaccum and Prospero, 1980; Prospero and Carlson, 1980; Prospero and Nees, 1986; Savoie *et al.*, 1987; Moulin *et al.*, 1997; Chiapello *et al.*, 1999; Prospero and Lamb, 2003; Ginoux *et al.*, 2004; Chiapello *et al.*, 2005; Prospero *et al.*, 2008; Trapp *et al.*, 2010]. Several studies focused on explaining this variability by linking the observed dust load with climate indices. For example, a qualitative

¹School of Marine and Atmospheric Science, State University of New York at Stony Brook, Stony Brook, New York, USA.

²Department of Atmospheric Sciences, University of Illinois at Urbana-Champaign, Urbana, Illinois, USA.

Corresponding author: O. M. Doherty, School of Marine and Atmospheric Science, State University of New York at Stony Brook, Stony Brook, NY 11794, USA. (odoherty@ic.sunysb.edu)

©2012. American Geophysical Union. All Rights Reserved.
0148-0227/12/2012JD017767

link relating mineral dust in Barbados and an El Niño-Southern Oscillation (ENSO) index has been suggested by *Prospero and Lamb* [2003]. *Moulin et al.* [1997] demonstrated a statistical relationship between mean annual dust load at Barbados and the mean value of the North Atlantic Oscillation (NAO) index, while *Chiapello and Moulin* [2002] linked variability in satellite observations of dust over the tropical North Atlantic Ocean off the coast of Africa to variability of the NAO during winter. *Ginoux et al.* [2004] showed a weak statistical relationship between the winter NAO index and the observed surface dust at Barbados as well as in simulated mineral dust concentration in the region. *Doherty et al.* [2008] demonstrated an improvement upon the relationship of NAO and mineral dust by showing an even stronger relationship between the location of the Azores High in the Atlantic and the Hawaiian High in the Pacific and dust in the Caribbean.

[5] In this work we present a new perspective on mineral dust transport in the region by focusing on the role of the Intertropical Convergence Zone (ITCZ) over Africa rather than on global teleconnections indices as has previously been done. Here we consider the ITCZ to represent the zone of near-surface convergence over continental West Africa that is sometimes referred to as the West African monsoon trough [*Sultan et al.*, 2003]. Year-to-year and decade-to-decade variability of the ITCZ has been observed over Africa and the Atlantic [*Mächel et al.*, 1998; *Kapala et al.*, 1998], with differences in the intensity and location noted. Some variability of the ITCZ can likely be ascribed to changes in sea surface temperature [*Folland et al.*, 1986; *Hoerling et al.*, 2006] as precipitation in the Sahel has been linked to sea surface temperature changes [*Folland et al.*, 1986; *Giannini et al.*, 2003]. *Tomas et al.* [1999] present theoretical evidence for the location of the ITCZ also being a function of the cross-equatorial pressure gradient.

[6] It has been previously noted that a relationship between the ITCZ and mineral dust likely exists. The trade wind circulation associated with the ITCZ blows through the area downwind of the Sahara and Sahel where mineral dust loads are the highest [*Prospero and Carlson*, 1972; *Moulin et al.*, 1997]. *Prospero and Carlson* [1972] first showed in a field experiment that the dust belt was located directly to the north of the ITCZ. *Moulin et al.* [1997] and later *Evan et al.* [2006b] showed using satellite observations of mineral dust that the dust belt moves north blowing dust into the Caribbean ahead of the ITCZ in summer, and returns south blowing dust into South America in winter. Precipitation in the tropical North Atlantic basin and surrounding locations have been shown to be dependent on the location of the ITCZ [*Kapala et al.*, 1998] and multiple studies have linked mineral dust in Barbados with precipitation in the Sahel region of Africa [*Prospero and Nees*, 1986; *Chiapello et al.*, 2005].

[7] Although work has been done linking the movement of the ITCZ to changes in dust load locally in Africa [*Engelstaedter and Washington*, 2007; *Schwanghart and Schütt*, 2008; *Sunnu et al.*, 2008; *Lau et al.*, 2009; *Wilcox et al.*, 2010], this is the first study that addresses how the movement of the ITCZ has implications for the amount of dust that extends over the Atlantic and reaches the Americas. Specifically we examine how changes in the ITCZ effect wind and precipitation patterns over both the North Africa and the Tropical North Atlantic and in turn control the amount of

mineral dust that reaches Barbados. We focus in this paper on the winter season to compare to more well known teleconnections such as the NAO and ENSO. Although less dust reaches Barbados in winter than does in summer [*Kaufman et al.*, 2005], dust continues to reach Barbados in winter in appreciable quantities as Barbados lies on the northern edge of this dust plume. The dustier summer season will be the focus of a forthcoming paper.

[8] The structure of this paper is as follows. In Section 2 we describe how we quantify the variability of the ITCZ. We will introduce the various data sets used in this study in Section 3. In Section 4 we will then explore the long-term relationship between mineral dust in Barbados and the ITCZ, and we will compare the physical mechanisms by which the ITCZ impact the mineral dust concentrations in Barbados. Section 5 concludes our findings.

2. The ITCZ Over West Africa as a Center of Action

[9] Year-to-year and decade-to-decade [*Mächel et al.*, 1998; *Kapala et al.*, 1998] variability of the ITCZ has been observed, with differences in the intensity and location noted. To compare to the record of mineral dust at Barbados, a time series of the position and intensity of the ITCZ is necessary. Here we develop such a time series by utilizing the “Center of Action” (COA) approach. This provides us with three indices, one for the latitudinal position, one for the longitudinal position, and one for the intensity of the system.

[10] The concept of an atmospheric “Centers of Action” (COA) was first suggested by *Rossby* [1939] and used by others since [*Angell and Korshover*, 1974, 1982; *Hurrell*, 1995; *Kapala et al.*, 1998; *Mächel et al.*, 1998]. A COA is a seasonal large-scale system which occurs annually in nearly the same geographic region. Examples of such COA are the Azores High COA or the Icelandic Low COA. While each of these COA have a well established and well understood long-term mean location, on a monthly or seasonal basis there is a large amount of variability in its exact location. As each of these COA are often the major climatic feature of a given region for a given season, this short-term location variability can be extremely important in terms of dictating the weather for a given season. Similarly each COA can vary in terms of its strength or intensity from month to month or season to season.

[11] Once the position and intensity is quantified by the COA indices, those indices can be related to geophysical variables to investigate their relationships. Such an approach in the midlatitudes has been successfully applied to many geophysical systems, e.g. solar cycle variability [*Christoforou and Hameed*, 1997], cloud cover and global temperature [*Croke et al.*, 1999], zooplankton in the Gulf of Maine [*Piontkovski and Hameed*, 2002], location of the Gulf Stream northwall [*Hameed and Piontkovski*, 2004], mineral dust transport [*Riemer et al.*, 2006; *Doherty et al.*, 2008], variability in sea level [*Kolker and Hameed*, 2007], frequency of Greenland tip jet events [*Bakalian et al.*, 2007] and sea-surface temperatures in the Gulf of Lion [*Jordi and Hameed*, 2009]. As we will describe shortly, in this paper we apply this framework to the ITCZ over West Africa.

[12] In the literature there is some ambiguity regarding the definition of the term ITCZ [*Nicholson*, 2009]. The term

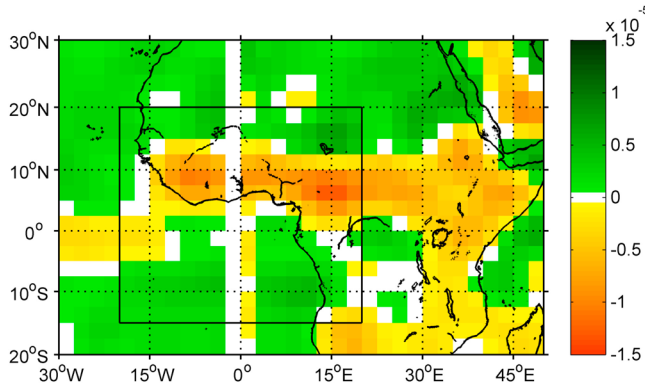


Figure 1. Mean winter (DJFM) divergence at 925 hPa as computed from NCEP Reanalysis winds. The box over which the WACZ COA is computed is shown in black.

ITCZ has been applied to both the tropical rain belt over West Africa [Sultan *et al.*, 2003] and the region of near-surface convergence, sometimes referred to as the Inter Tropical Front (ITF). As explained below, we define our index of convergence to be the center of mass of the low level (925 hPa) convergence as described in NCEP Reanalysis over West Africa. We refer to this as the West Africa Convergence Zone (WACZ) to avoid any confusion with terminology associated with the ITCZ in the literature. Defined in this way, the WACZ is observed to be north of the African Easterly Jet as described in Mohr and Thorncroft [2006], consistent with the conceptual model presented in Nicholson [2009]. It is shown to be associated with large scale changes in circulation and precipitation both locally in West Africa and regionally over the Tropical Atlantic.

[13] While pressure has previously been used as the field to quantify the COA [Hameed and Piontkovski, 2004; Riemer *et al.*, 2006; Doherty *et al.*, 2008], in the tropics the gradient of sea level pressure is very small, and so we follow after Kapala *et al.* [1998] and use divergence as the reference field. Specifically, we define the WACZ to be the center of mass of the low level (925 hPa) convergence as described in NCEP Reanalysis [Kalnay *et al.*, 1996] over West Africa (15°S to 20°N and 20°W to 20°E). Figure 1 shows the climatological mean of divergence at 925 hPa from NCEP Reanalysis from 1965–2003 during the boreal winter including the months December to March. The three WACZ COA indices identify the position and intensity of the center of mass of the band of convergence extending between 5°N and 10°N from the West African coast east across the continent.

[14] The intensity index W_i is defined as an area-weighted divergence departure from a threshold value over the domain (I, J)

$$W_i = \frac{\sum_{i,j=1}^{I,J} (D_{i,j} - D_t) \cos \phi_{i,j} (-1)^M \delta_{i,j}}{\sum_{i,j=1}^{I,J} \cos \phi_{i,j} \delta_{i,j}}, \quad (1)$$

where $D_{i,j}$ is the divergence value at 925 hPa at a grid point (i, j) , D_t is the threshold divergence value ($D_t = -1.8 \times 10^{-6} \text{ s}^{-1}$), $\phi_{i,j}$ is the latitude of grid point (i, j) , $M = 0$ for divergent systems and 1 for convergent systems, $\delta = 1$ if $(-1)^M (D_{i,j} - D_t) > 0$, and $\delta = 0$ if $(-1)^M (D_{i,j} - D_t) < 0$.

[15] The latitudinal index W_ϕ is defined as:

$$W_\phi = \frac{\sum_{i,j=1}^{I,J} (D_{i,j} - D_t) \phi_{i,j} \cos \phi_{i,j} (-1)^M \delta_{i,j}}{\sum_{i,j=1}^{I,J} (D_{i,j} - D_t) \cos \phi_{i,j} (-1)^M \delta_{i,j}}. \quad (2)$$

The longitudinal index W_λ is defined analogously. The location indices thus give divergence-weighted mean latitudinal and longitudinal positions of the WACZ.

[16] As a result we obtain time series of monthly values for latitude (W_ϕ), longitude (W_λ) and intensity (W_i) that characterize the WACZ. The indices are available from January 1948 to the present. Results were not significantly sensitive to changes in box size, the box location or the divergence threshold. This work focuses on the seasonal variability of mineral dust and the WACZ in boreal winter, and to represent this we use the average of four months December ($Y - 1$), January (Y), February (Y) and March (Y) where Y represents the year of the winter season. Our choice of DJFM is motivated by the work of Ben-Ami *et al.* [2011] who find that dust transport of Africa enters its southerly or winter mode from the end of November through the end of March. Values of the WACZ presented in this work are for the period December 1965 to March 2003, concurrent with the mineral dust record at the surface.

3. Data Sets

[17] In this study we utilize the mass concentration of mineral dust as recorded in Barbados. Barbados is an ideal location for observing mineral dust as it is the first landmass encountered by mineral dust traveling over the North Atlantic from Africa. Mineral dust at the surface at Barbados has been the subject of previous studies [Prospero *et al.*, 1970; Carlson and Prospero, 1972; Prospero and Nees, 1986; Moulin *et al.*, 1997; Prospero and Lamb, 2003; Ginoux *et al.*, 2004; Chiapello *et al.*, 2005] and is the longest continuous record of surface mineral dust concentrations. The record of monthly mineral dust at Barbados is available from August 1965 through December 2003. Data is collected near the surface at Barbados, located at 13°10'N and 50°30'W.

[18] We use NCEP/NCAR Reanalysis wind data from NOAA/ESRL PSD [Kalnay *et al.*, 1996] to calculate the WACZ COA indices. Data is available from January 1948 to present, although we only consider the period of 1965–2003 to be consistent with the mineral dust record at Barbados. We compared the WACZ COA index from NCEP/NCAR Reanalysis to one calculated from ERA-40 (not shown), and for the winter season we found the two were not statistically different. NCEP/NCAR Reanalysis winds were also used to compute composite images, as described in Section 4.2.

[19] Two traditional teleconnection climate indices are used in this study for comparison purposes, the NAO and ENSO. Monthly values of the NAO are from the Climate Prediction Center of NCEP/NOAA (<http://www.cpc.ncep.noaa.gov>). ENSO monthly values are also from the Climate Predictions Center of NCEP/NOAA who computes the ENSO indices from NOAA OI SST product over multiple regions in the Pacific.

[20] The GPCP Data set (v 2.1) [Adler *et al.*, 2003] is used for precipitation data in this study. Data is available from January 1979–April 2008, however data after 2003 is not

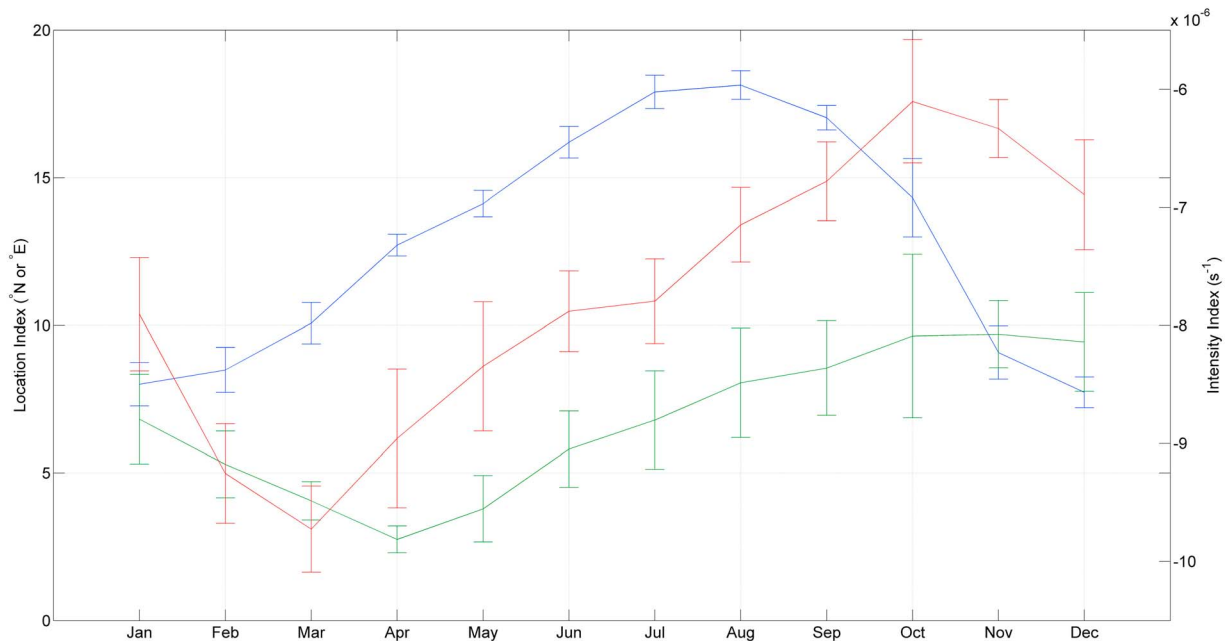


Figure 2. The long-term mean (1965–2003) of the WACZ latitude (W_ϕ) (blue line, left axis), longitude (W_λ) (green line, left axis) and intensity (W_i) (red line, right axis). Error bars represent the standard deviation based on the monthly average for each index.

used in this study to be consistent with the mineral dust record at Barbados.

[21] We use TOMS Aerosol Index (AI, v 8.0) as a measure of aerosol load [Herman *et al.*, 1997]. Data is available for the period 1979–1993 and 1996–2005. As described in Kiss *et al.* [2007] some calibration and instrument errors exist for this instrument. To this end we do not use the AI in any quantitative way, but present it as a qualitative aid in understanding how dust load changes with variation in the WACZ.

4. Results

4.1. Climatology of West Africa Convergence Zone

[22] As shown in Figure 2 the WACZ (as defined in Section 2) displays a clear seasonal latitudinal migration from its southernmost point in January to its northernmost point in August. The latitudinal index W_ϕ is thus consistent with the conventional understanding that the WACZ's location is seasonal and that the WACZ moves to follow the solar heating [Folland *et al.*, 1991]. The index W_ϕ reaches its northernmost position over Africa in July and August, trailing the movement of the solar heating maxima by one to two months. Nicholson [2009] notes that August also represents the period of maximum rainfall in the Sahel region and the period of maximum variability associated with the WACZ.

[23] The movement of the WACZ is not a simple north-south migration, but rather is a two-dimensional migration. W_λ reaches its most westward point in the spring and moves toward the east in the fall. Coupled with the annual latitudinal migration, this means the WACZ moves on a NW to SE axis from spring/summer into fall/winter. Maximal convergence occurs in the spring and decreases to a minimum in fall, and is thus more intense in its north and west mode than its south and east mode.

[24] While the long-term mean of the indices shows a clear annual cycle with an obvious seasonal migration, both the inter- and intra-annual variability of the WACZ is large. In the summer, when W_ϕ reaches its northernmost maximum there are large differences in the latitudinal position from year to year, ranging from 16 to 19 degrees north. In semi-arid locations such as the Sahel, a large shift in the location of the WACZ can be the difference between flooding and drought, and in turn can greatly effect soil conditions and ultimately dust mobilization. Additionally the latitudinal intra-annual variability plays a major role in controlling regional climate. Some years the WACZ remained in a northward phase for multiple consecutive months, leading to an extended rainy season for the Sahel, while in other years the northward phase and hence the rainy season is very short. The duration of the northward rainy phase may be critical in determining soil characteristics for the semi-arid Sahel, particularly in the summer when strong solar insolation can quickly dry out soils.

4.2. Relationship of Mineral Dust at Barbados and WACZ and ENSO During Winter

[25] To establish a relationship we correlated mean winter (DJFM) dust load at Barbados with the mean winter (DJFM) WACZ COA indices (W_ϕ , W_λ and W_i). Winter season mineral dust load at Barbados is significantly correlated with the location of the WACZ in terms of both the latitude (W_ϕ) and longitude (W_λ) of the WACZ at an α of at least 0.01 as shown in Table 1. No statistical relationship between the intensity of the WACZ (W_i) and mineral dust at Barbados was observed. Since the W_ϕ index increases in value as the WACZ moves north, the negative correlation observed between dust and W_ϕ suggests that as the WACZ moves south dust load at Barbados increases. Likewise the positive correlation between dust and W_λ suggests that as the WACZ moves eastward dust load at Barbados increases.

Table 1. Spearman Rank Correlation Coefficients Between Mean DJFM Mineral Dust at Barbados and Climate Indices for DJFM Season 1965 to 2003

| | W_ϕ | W_λ | W_i | NAO | E_{1+2} | E_3 | E_4 | $E_{3,4}$ |
|------------------|--------------------|-------------------|-------|------|-------------------|-------|-------|-----------|
| Dust at Barbados | -0.69 ^a | 0.51 ^b | -0.13 | 0.18 | 0.30 ^c | 0.18 | 0.11 | 0.15 |

^aSignificance at <0.001.^bSignificance at 1%.^cSignificance at 5%.

[26] Traditionally a Pearson product-moment correlation coefficient is used to represent covariance between two data sets. The Pearson product-moment correlation coefficient is not robust as it requires a normal distribution for both data sets nor resistant to outliers [Wilks, 1995]. Both the seasonally mean DJFM mineral dust at Barbados and ENSO climate indices used in this work are not normally distributed, and in the case of the ENSO data set include multiple outliers. To reduce the impacts of outliers between data sets we use the Spearman rank correlation as shown in Wilks [1995]. It should be noted that using either the Pearson or the Spearman correlation coefficients the correlations between dust and W_ϕ , W_λ and E_{1+2} are statistically significant, but the Spearman correlation coefficient gives a more representative reflection of the covariance between data sets.

[27] The indices W_ϕ and W_λ are not independent of one another as shown in Table 2. The WACZ is located further east in winters when it is in its south phase, and further west in winters when it is in its north phase, suggesting that in the winter season the WACZ varies along a NW to SE axis. This NW to SE axis is clearly visible in Figure 3a where during seasons in which the WACZ is north (blue diamonds) it also tends to be west and vice versa. Hence the NW location correlates to a reduction of mineral dust in Barbados and the SE location correlates to an increase in mineral dust at Barbados. Figure 3b shows the magnitude of change in divergence at 925 hPa that accompanies the NW to SE shift, and a clear dipole pattern emerges. To produce this figure we subtracted the seasonal winter mean (DJFM) of divergence of the northernmost WACZ seasons (75th percentile) from the seasonal winter mean (DJFM) of the southernmost WACZ seasons (25th percentile). The black contour indicates a significant difference at 10%. The box over which the WACZ COA is computed is shown in black.

[28] Figure 4 shows the temporal relationship between W_ϕ and mineral dust load at Barbados. Mineral dust load at Barbados reached its lowest value during the mid-1960's when W_ϕ is found to be at its most northward location, and it reached its peak in the mid-1980's when W_ϕ was in its most southward location.

[29] Also shown in Table 1 is that the south and east migration of the WACZ explains more of the variability of the mineral dust than traditional climate indices such as the NAO or ENSO do. The ENSO Region 1+2 (E_{1+2}) is located along the coastline of Ecuador and Peru, ENSO 3 (E_3) is located just to the north and west of ENSO 1+2 spanning the central Pacific, and ENSO 4 (E_4) is the westernmost box approaching Papua New Guinea. We observe that the largest correlation between mineral dust and ENSO occurs for the ENSO index closest to South America (E_{1+2}), with the correlation coefficient attenuating moving into the Central

Pacific. The relationship between ENSO and mineral dust is statistically significant at 5% close to the coast of South America (E_{1+2}) and not significant for the eastern Pacific (E_3), central Pacific ($E_{3,4}$) and central-west Pacific (E_4). This is consistent with Mahowald *et al.* [2003] who did not find widespread correlations in and around West Africa between dust and $E_{3,4}$ using a combination of modeling results and station observations. Our results suggest that statistical correlations between mineral dust transport and ENSO are sensitive to choice of ENSO domain.

[30] As E_{1+2} and W_ϕ are not independent ($r = 0.80$), we apply a partial correlation analysis to account for their covariance and assess the relationship between each and mineral dust as if they were independent [Wilks, 1995]. There is precedent for using a partial correlation analysis to remove an ENSO signal. Sankar-Rao *et al.* [1996] use partial correlation to evaluate the signal of the Indian Monsoon on Eurasian seasonal snowfall without the influence of ENSO. More recently partial correlation was used similarly in a paper on mineral dust, tropical cyclone activity and ENSO [Evan *et al.*, 2006a]. If we evaluate the rank correlation between mineral dust and W_ϕ with E_{1+2} held constant, the correlation coefficient decreases only slightly from $r = -0.69$ to $r = -0.66$, remaining significant at α of <0.001. The rank correlation between mineral dust and E_{1+2} with W_ϕ held constant decreases from $r = 0.30$ to $r = 0.06$, which is statistically insignificant. Much of the statistical relationship between E_{1+2} and mineral dust is a mathematical artifact caused from E_{1+2} varying in time with W_ϕ . We confirmed this in a separate composite analysis and find no physical relationship between E_{1+2} and wind or precipitation over emission, transport and deposition regions (not shown).

[31] To corroborate our findings on the statistical relationships of Barbados mineral dust and the WACZ, we present the appropriate composite figures of the TOMS Aerosol Index (AI) data from NIMBUS-7 (1979–1993) and Earth Probe (1996–2005) as a semi-quantitative proxy for dust load over the entire Tropical North Atlantic. We analyze AI data to assess if the relationship between the WACZ and mineral dust at Barbados is reflective of larger scale changes in mineral dust load over the North Atlantic and Caribbean. AI measures absorbing particles in the atmosphere by comparing observed UV measurements to an idealized UV profile of the atmosphere. TOMS AI is not able to differentiate between types of absorbing aerosols, in particular particles from biomass burning register similarly to mineral dust aerosols. During boreal winter biomass burning is at a maximum [Formenti *et al.*, 2008] in North Africa, and a mix of mineral dust and biomass burning aerosols are likely. TOMS AI has known biases due to the height of the aerosol layer [Herman *et al.*, 1997; Mahowald and Dufresne, 2004], calibration drift errors [Kiss *et al.*, 2007] and cloud contamination

Table 2. Cross Correlation Spearman Rank Coefficient Between Mean Winter (DJFM) WACZ COA Indices for DJFM Season 1965 to 2003

| | W_ϕ | W_λ | W_i |
|-------------|--------------------|--------------------|-------|
| W_ϕ | - | -0.73 ^a | -0.08 |
| W_λ | -0.73 ^a | - | 0.06 |
| W_i | -0.08 | 0.06 | - |

^aStatistical significance at $\alpha < 0.001$.

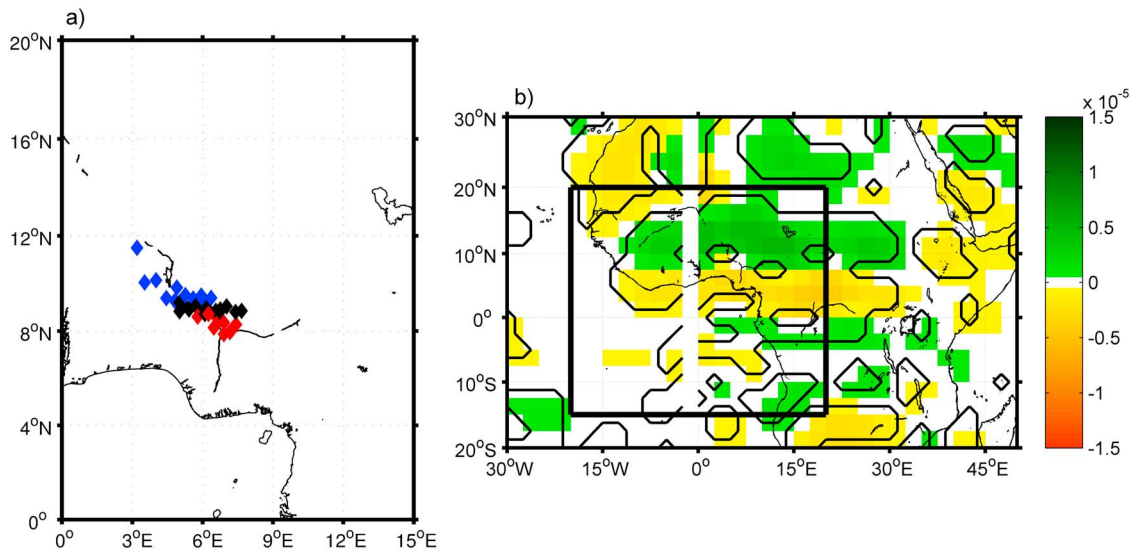


Figure 3. (a) Location of seasonal winter (DJFM) mean of WACZ COA over the period 1965 to 2003. Blue dots represent the northern (75th percentile) phase of WACZ COA, red dots represent southern (25th percentile) phase of WACZ COA. Black dots represent the middle 50 percent seasons of WACZ COA. (b) Difference in divergence of NCEP Reanalysis at 925 hPa during winter (DJFM) over the period 1965 to 2003. Differences are calculated by subtracting the seasonal winter mean (DJFM) of the northern most WACZ seasons (75th percentile) from the seasonal winter mean (DJFM) of southern most WACZ seasons (25th percentile). The difference represents the conditions of the WACZ latitude index for which dust is maximized at Barbados. Black contour represent a significant difference at 10%. The box over which the WACZ COA is computed is shown in black.

issues [Torres et al., 1998, 2002]. Here we only seek to verify the relationships of mineral dust surface observation and WACZ index, and so a qualitative use of the TOMS data is appropriate.

[32] We use composites to represent seasonal conditions in which an index is in a positive or negative phase. The index

W_ϕ is ranked in ascending order, the lowest quartile (q25) of data is identified as the negative phase and the highest quartile (q75) of data is identified as the positive phase. The years used to compute the seasonal composites are shown in Table 3. For W_ϕ the negative phase (q25) corresponds to periods in which the WACZ is in a south mode, and

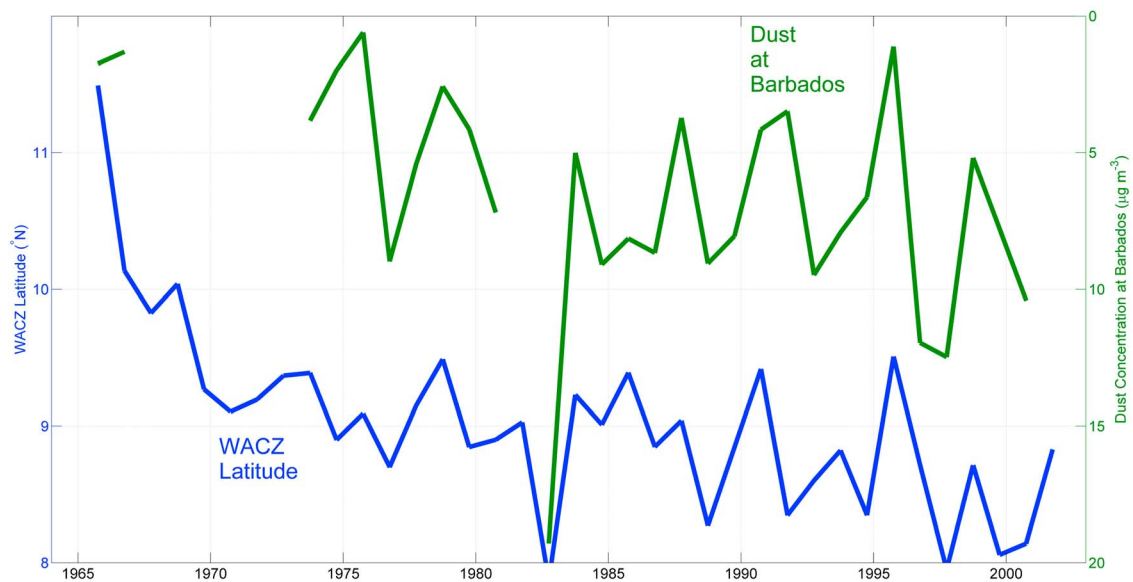


Figure 4. Comparison of the position of the mean DJFM WACZ latitude (left axis) and mean DJFM dust load at Barbados (right axis, inverted) over the period 1965 to 2003. Seasonal averages are calculated only for seasons that contain concentration data for all months of the season. Both time series are averaged over the winter months of December–March.

Table 3. Years That Were Used to Generate Seasonal Mean Composite Images of AI, Wind and Precipitation Based on W_{ϕ} ^a

| | q25 | q75 |
|---------------|--|--|
| AI | 1983, 1998, 1989, 1992, 2000, 2001 | 1984, 1985, 1986, 1988, 1991 |
| Wind | 1977, 1983, 1989, 1992, 1993, 1995, 1998, 1999, 2000, 2001 | 1966, 1967, 1968, 1969, 1973, 1974, 1979, 1986, 1991, 1996 |
| Precipitation | 1983, 1989, 1992, 1998, 2000, 2001 | 1982, 1984, 1986, 1988, 1991, 1996 |

^aEach season mean was calculated using the average of four individual months of data; December ($Y - 1$), January (Y), February (Y) and March (Y) where Y represents the year of the winter season.

the positive phase (q75) corresponds to periods in which the WACZ is in a north mode. All seasons of AI data that have been selected as negative (q25) or positive (q75) phases are then averaged together to form a composite.

[33] Figure 5 shows composites of TOMS AI with respect to the northward (minimum dust in Barbados) and southward phase (maximum dust at Barbados) of W_{ϕ} . We restrict our analysis to the period 1979–1993, 1996–2003 to included all AI data that is concurrent with the dust record at Barbados. Barbados is observed to be in a plume of dust entering the Caribbean in the southward phase of the WACZ (Figure 5a). When the WACZ is south (Figure 5a), the greatest values of AI occur between 15° and 20°N, from the Atlantic Coastline east to 20°E. A very large plume of mineral dust is also evident over the Tropical North Atlantic centered between 15° and 20°N, which extends into the Caribbean Sea. The largest AI values of greater than AI = 3.0 occur near the Bodele Depression, a known hot spot for mineral dust emission in Africa [Washington *et al.*, 2003]. Along the Gulf of Guinea values of AI are modest, near AI = 1.0 and likely reflect a mix of mineral dust and biomass burning aerosols.

[34] In contrast, when W_{ϕ} is in its northward phase, the highest values of AI occur along the Gulf of Guinea, extending westward into the Tropical North Atlantic, centered at about 7.5°N. While some of this plume may be the result of biomass burning, Formenti *et al.* [2008] found that more than 70% of this material is mineral dust. A peak in AI (AI = 2.5) is observed near the Bodele Depression. Over much of the Sahara values of AI are modest, coming in around 1.0.

[35] Comparing the north and south phases of the WACZ, a clear dipole in AI is evident in the composite difference image (Figure 5c), similar to the dipole pattern in the composite difference for divergence as shown in Figure 3b. As the WACZ moves southward a large increase in AI is seen over the Sahara Desert, with increasing value of AI extending over a broad geographical area northward to the Mediterranean and eastward to the Red Sea, suggesting a robust response in dust emission to southward movement of the WACZ.

[36] Higher values of AI are observed across nearly all of the Tropical North Atlantic north of 10°N suggesting a large increase in westward transport of mineral dust. Increases in AI are visible into the Caribbean. This analysis supports the conclusion drawn from the observed correlations, that mineral dust at the surface at Barbados increases as the WACZ moves southward.

[37] Over Africa south of the Sahel and in particular south of 12°N a decrease in AI is observed as the WACZ moves southward. It is not clear if this is due to a decrease in mineral dust transport into this region or a reduction in biomass

burning aerosols as TOMS AI cannot differentiate between mineral dust and biomass burning aerosols. This reduction in AI over this region is not likely due to precipitation as DJFM is the dry season in the Sahel, where precipitation is very low.

[38] Our results are similar to those of Engelstaedter and Washington [2007] who find a spatial correlation between 10 m-divergence in ERA-40 and TOMS-AI over much of North Africa. Our results differ from the findings of Ben-Ami *et al.* [2011] who argue that during the boreal winter season that the dust plume across the Atlantic is constrained to a band centered on 4°N. However, when the WACZ is in its north phase our results support the finding of Ben-Ami *et al.* [2011] as maximum aerosol load does appears to be near 4°N. We find that the location of the dust belt in TOMS-AI measurements is sensitive to the latitudinal position of the WACZ during the boreal winter, shifting northward to include Saharan sources when the WACZ is south phase. We find a plume of most likely mixed dust-biomass smoke is found near to 4°N only when the WACZ is in a north phase. It should be noted that the studies focus on different time periods. This analysis includes years over the period 1979–1993/1996–2004, whereas the Ben-Ami data is from the 21st century only.

4.3. Physical Mechanisms for Observed Correlation

[39] The strong correlation between W_{ϕ} and mineral dust at Barbados and mineral dust at Barbados must be explained physically. Next we will examine how changes in W_{ϕ} impact wind and precipitation in the region, which in turn control the emission and transport of mineral dust from the Sahara.

[40] Strong northeast winds over the Sahel have been shown to increase mineral dust emissions [Engelstaedter and Washington, 2007; Schwanghart and Schütt, 2008; Doherty *et al.*, 2008]. Figure 6 shows the composite difference in winds for the 25th percentile W_{ϕ} (southern most) winter (DJFM) seasons minus the 75th percentile W_{ϕ} (northern most) winter (DJFM) seasons over the period December 1965–March 2003. This represents the difference in flow from the southern mode in which mineral dust is maximized at Barbados and the northern mode in which such dust is minimized. Figure 6a shows a strengthening of near-surface northeasterly winds during these conditions. This strengthening occurs over much of the Sahel and the Eastern Sahara, which are important source regions for mineral dust [Washington and Todd, 2005; Engelstaedter and Washington, 2007]. We hypothesize that the location of these strengthening winds is important in increasing dust emissions.

[41] Northeastern winds in this region are typical in winter [Engelstaedter and Washington, 2007]. These winds known

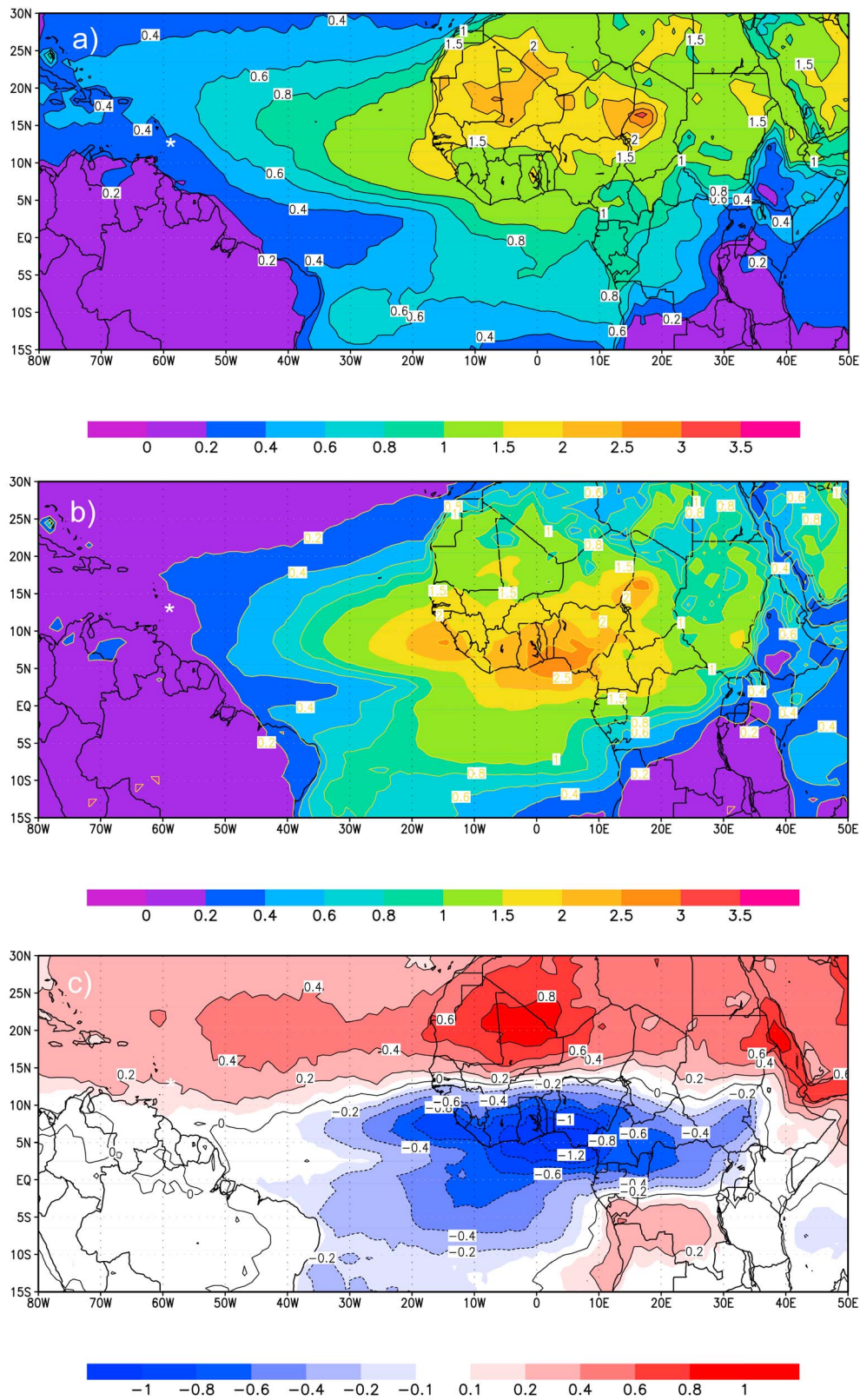


Figure 5. (a) Composite mean of TOMS AI for the southernmost winter (DJFM) seasons (25th percentile) of the WACZ. (b) As in Figure 5a but for the northernmost WACZ latitude (75th percentile) winter (DJFM) seasons. Seasons with missing AI data are excluded from the composite. (c) The difference of Figure 5a minus Figure 5b, i.e. conditions of the WACZ latitude index for which dust load is maximized at Barbados. All composites are calculated over the period 1979–93; 1996–2003. Asterisks represent the location of Barbados.

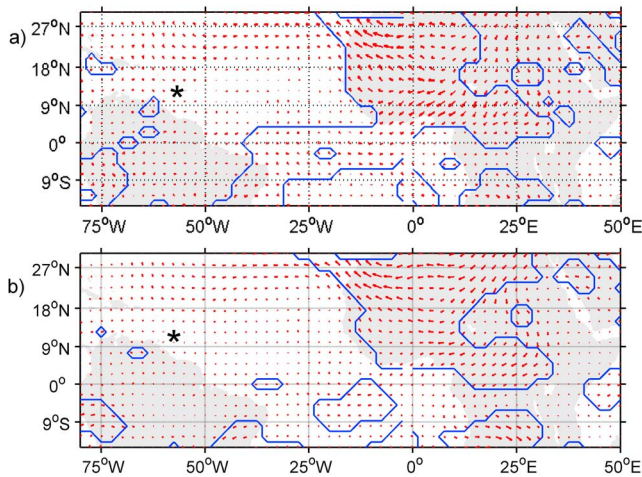


Figure 6. Difference in composite mean of NCEP Reanalysis winds at (a) 925 hPa and (b) 850 hPa. Differences are calculated by subtracting the seasonal winter mean (DJFM) of the northern most WACZ seasons (75th percentile) from the seasonal winter mean (DJFM) of southern most WACZ seasons (25th percentile). The difference represents the conditions of the WACZ latitude index for which dust is maximized at Barbados. All composites are calculated over the period 1965–2003; Blue contour represent a significant difference at 10%. Asterisks represent the location of Barbados.

as the Harmattan winds transport mineral dust from the Sahara and Sahel regions southwards into sub-Saharan Africa in winter. The Harmattan winds are effective at emitting dust not only because of their strength but because of where they occur. The area around Lake Chad is a major source of mineral dust emissions [Washington and Todd, 2005] and just downwind of this region the largest increase in north-eastern flow (Figures 6a and 6b) is observed as the WACZ changes phase. Ben-Ami et al. [2011] suggest that the Bodele Depression, which lies just north and east of Lake Chad, is the primary source of mineral dust during the boreal winter, where dust emissions are highly dependent on near-surface wind speeds [Koren and Kaufman, 2004]. Again near to the Bodele Depression we note increases in NE winds as the WACZ changes phase.

[42] Our results support the hypothesis of Schwanghart and Schütt [2008] who noted the role of Harmattan winds which blow over the Bodele Depression, emitting large quantities of mineral dust in the boreal winter. In their study, Schwanghart and Schütt [2008] observed that the strength of NE winds at 850 and 925 hPa near the Bodele was tightly correlated to the amount of mineral dust emitted in winter. Schwanghart and Schütt [2008] suggested that northward movement of the ITCZ had the capacity to diminish the NE winds. Our results here confirm their hypothesis.

[43] In summary the strength of the NE Harmattan winds are an important control on the amount of mineral dust that is emitted in the boreal winter. We hypothesize that shifts in the WACZ controls dust emission not only by increasing wind speeds over much of West Africa, but does so by focusing these increases in critical locations such as the

Sahel, Lake Chad and the Bodele Depression. Similar near-surface wind increases are observed from the composites for W_λ (not shown).

[44] Steering winds aloft at the base of the Saharan Air Layer show an increase in east to west flow, increasing trans-Atlantic transport of emitted particles (Figure 6b). The height of the Saharan Air Layer depends on the season [Carlson and Prospero, 1972], and satellite observations suggest that mineral dust transport is constrained to heights below 700 hPa in boreal winter over the Tropical North Atlantic [Ben-Ami et al., 2009]. Figures 6a and 6b both show an increase in trans-Atlantic transport, although this increase is not statistically significant.

[45] Figure 7a shows the winter (DJFM) mean precipitation for years in which the WACZ is in its south phase. Maximum precipitation rates are observed south of the equator, with the highest values observed in Brazil south of the Amazon River. In Africa precipitation is highest in Central Africa, south of the equator. Moderate precipitation is observed between the equator and 9°N over West Africa. No precipitation occurs over the Sahel or Sahara, as winter is the dry season. Differences in precipitation between the south phase conditions of the WACZ (Figure 7a) and the north phase conditions are shown in Figure 7a. Composite differences are calculated in such a way to show conditions that lead to maximized dust load at Barbados. We do not see a shift in the location of precipitation as the phase of W_ϕ changes, but rather a large scale drying across the Central Africa, the equatorial Atlantic and the Amazon Basin.

[46] Precipitation over mineral dust source regions is not affected by changes in W_ϕ . No change in the amount of precipitation over the Sahel or Sahara regions occurs as W_ϕ changes phase from south to north, as no precipitation falls

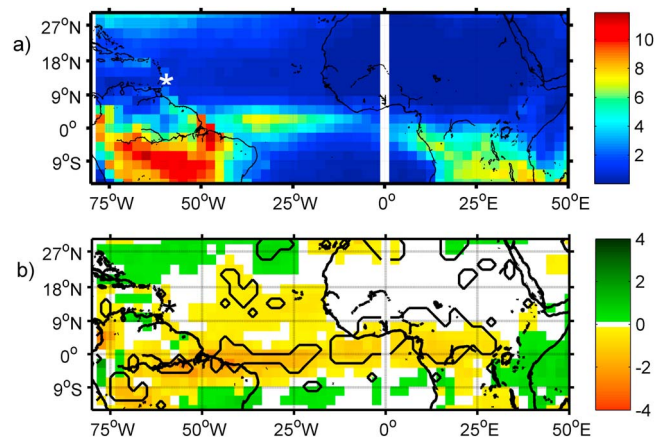


Figure 7. (a) Composite mean of GPCP precipitation for the southernmost winter (DJFM) seasons (25th percentile) of the WACZ over the period 1979 to 2003. (b) Difference in composite mean of GPCP precipitation over the period 1979 to 2003. Differences are calculated by subtracting the seasonal winter mean (DJFM) of the northern most WACZ seasons (75th percentile) from the seasonal winter mean (DJFM) of southern most WACZ seasons (25th percentile). The difference represents the conditions of the WACZ latitude index for which dust is maximized at Barbados. Black contour represent a significant difference at 10%. Units are mm day^{-1} from GPCP. Asterisks represent the location of Barbados.

Table 4. Years That Were Used to Generate Seasonal Mean Composite Images Wind and Precipitation Based on W_i^a

| | q25 | q75 |
|---------------|--|--|
| Wind | 1996, 1990, 1995, 1968, 1985, 1981, 1984, 1989, 1997, 1970 | 1969, 1967, 2003, 1966, 1999, 2000, 2002, 1979, 1998, 1992 |
| Precipitation | 1996, 1990, 1995, 1985, 1981, 1984 | 2003, 1999, 2000, 2002, 1998, 1992 |

^aEach season mean was calculated using the average of four individual months of data; December ($Y - 1$), January (Y), February (Y) and March (Y) where Y represents the year of the winter season.

in this region during either phase. Wet deposition, vegetation, soil moisture in source regions are therefore not related to W_ϕ in winter.

[47] In contrast to the Sahel and Sahara, over the tropical North Atlantic Ocean precipitation is non-zero. Mineral dust reaching Barbados and the Caribbean encounters precipitation in these regions as it is transported. Figure 7b suggests that dust maximization at Barbados is consistent with drier conditions in the tropical North Atlantic region, however. Although dust transport to the Americas could be increased in seasons when W_ϕ is in its south phase as less precipitation and therefore less wet deposition occurs, the observed change in precipitation here is too small to support this conclusion. Based on changes in precipitation in source and transit regions we conclude that changes in precipitation driven by variability W_ϕ are not important for mineral dust emission and transport to Barbados. Interestingly, Figure 7 shows significant precipitation occurring during the winter season across the equatorial Atlantic into South America, suggesting the wet deposition may be an important removal process in this region. As the W_ϕ changes to the southern phase, significant drying is observed across the equatorial Atlantic into South America (Figure 7b). While this is not relevant for the dust transport processes that are the focus of this paper, we hypothesize that this drying would reduce wet deposition of mineral dust that is transported to the Amazon Basin during winter from the Sahara and Sahel by way of the equatorial Atlantic (Figure 5).

[48] Table 1 shows the near-zero correlation coefficient between intensity of WACZ (W_i) and mineral dust at Barbados ($r = 0.13$). This finding may seem surprising and counterintuitive, hence deserves further analysis. For this “null case” we produced composite images as was done for the latitude index W_ϕ . The weak (q25 of W_i) and intense (q75 of W_i) years used in these composite images are listed in Table 4. Here we note that since the correlation coefficient between W_i and dust at Barbados is near zero, the direction of the difference has no physical meaning. This is in contrast to the composites based on W_ϕ , which were built to highlight conditions that lead to dust maximization at Barbados.

[49] The differences in the wind field at both 925 hPa (Figure 8a) and 850 hPa (Figure 8b) are not statistically significant between intense and weak WACZ seasons over source regions of the Sahel or Sahara. Over the Tropical North Atlantic a few patches of increased east to west flow are observed, suggesting a slight increase in transport when the WACZ is weak compared to the strong phase. These patches of increased flow do not appear to be large enough in scale to increase mineral dust transport to Barbados. We attribute a lack of change in wind over source regions as an explanation for why the intensity of the WACZ is not correlated with mineral dust load at Barbados.

[50] As no precipitation falls in the source regions of the Sahel and Sahara and winter, the strength of the WACZ does not impact precipitation in these regions. Mineral dust emission is thus not impacted via precipitation as a function of WACZ intensity. Over the Tropical North Atlantic a general increase in precipitation is observed in years in which the WACZ is weak, with significant changes observed near to the African coastline. Mineral dust being transported to the Caribbean and Barbados could encounter more precipitation, and thus be impacted by wet deposition. Large changes in precipitation are observed over the equatorial Atlantic and Amazon Basin. Here precipitation is increased in the weak WACZ phase, potentially increasing removal of mineral dust via wet deposition.

[51] To summarize we observe no changes in near surface flow or precipitation over the source regions of the Sahel and Sahara as the WACZ changes phase from weak to strong. Hence no physical mechanisms for increased dust emission are tied to changes in the WACZ intensity. We do observe some changes in the transport region of the tropical North Atlantic Ocean, specifically favorable winds for transport are increased while removal by precipitation also increases in the weak phase of the WACZ. We conclude that (1) processes in the source region are more important than processes in the transport region for mineral dust transport to Barbados and the Caribbean and (2) increased transport via enhanced advection is compensated for by increased removal in the weak phase resulting in no significant change in transport.

[52] In summary, we note that increases in dust at Barbados during the winter season are associated with the WACZ moving south and that the underlying physical process is a change in winds in particular over the source region, not a change in precipitation. This is in agreement with the findings of *Sunnu et al.* [2008] who performed a field experiment and observed increased concentrations of mineral dust at the surface in Ghana when the ITCZ was south of the observing station in boreal winter.

5. Conclusions

[53] The relationship between convergence over West Africa, referred to as the ITCZ or West Africa Monsoon, and mineral dust in the Tropical North Atlantic has long been discussed, and in this paper we quantified the relationship for the winter season. We constructed three climate indices that quantify the variability of the convergence over West Africa by applying the Centers of Action approach to wind divergence at 925 hPa from NCEP Reanalysis. We demonstrated the utility of such indices by relating them to the

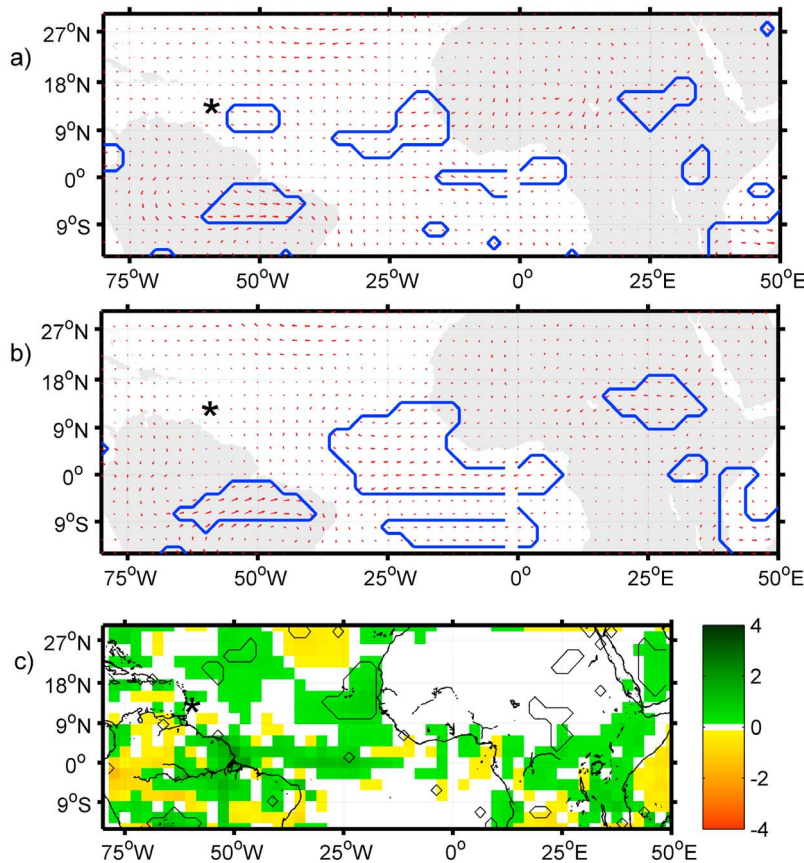


Figure 8. Difference in composite mean of NCEP Reanalysis winds at (a) 925 hPa and (b) 850 hPa. Differences are calculated by subtracting the seasonal winter mean (DJFM) of the weakest WACZ seasons (75th percentile) from the seasonal winter mean (DJFM) of strongest WACZ seasons (25th percentile). Wind composites are calculated over the period 1965–2003; Blue contour lines represent a significant difference at 10%. (c) Same as Figures 8a and 8b but for GPCP precipitation (mm day^{-1}) over the period 1979 to 2003. Black contour lines represent a significant difference at 10%. Asterisks represent the location of Barbados.

quantity of mineral dust reaching Barbados over the period from 1965 to 2003.

[54] Southward and eastward movement of the WACZ is associated with an increase of the quantity of mineral dust reaching the surface at Barbados. This increase can be explained by increases in near-surface NE Harmattan winds over the Sahel. The location of the increase in wind is critical with increases in NE flow observed near the key Lake Chad and Bodele Depression region. Combined this leads to increases in emission of mineral dust when the WACZ is in its south phase. Once emitted, mineral dust aerosols encounter an increase in the east-to-west trade wind flow over across much of the Saharan Air Layer over West Africa. This increase in advective flow could increase mineral dust transport toward the Americas.

[55] The latitude of the WACZ does not change dust emission or transport in winter by precipitation-driven effects. No changes in precipitation over the source regions of the Sahel or Sahara are noted, nor are significant changes observed in the transport zone between West Africa and

Barbados. Although not related to transport of mineral dust to Barbados, we note a distinct drying over much of Central Africa, the tropical Atlantic and parts of South America associated with southward movement of the WACZ.

[56] No relationship between the intensity of the WACZ and mineral dust was observed. We note that wind strength and direction does not change over key source regions between intense and weak phases of the WACZ. We hypothesize that this lack of change in winds explains why no relationship is observed between intensity of WACZ and mineral dust at Barbados. Although not related to transport of mineral dust to Barbados, weakening of the WACZ over Africa is shown to lead to drying over the equatorial Atlantic and Amazon Basin.

[57] Studies looking for links between naturally varying systems and the atmosphere often refer to familiar indices such as for example the NAO or ENSO. We show that the location and intensity of the WACZ is a strong alternative to other common indices, with clear links to changes in circulation in the region.

[58] **Acknowledgments.** We acknowledge and thank Joe Prospero and his staff for producing and sharing the record of mineral dust concentrations at Barbados. NCEP Reanalysis and GPCP Precipitation data provided by the NOAA/OAR/ESRL PSD, Boulder, Colorado, USA, from their Web site at <http://www.esrl.noaa.gov/psd>.

References

- Adler, R. F., et al. (2003), The Version-2 Global Precipitation Climatology Project (GPCP) monthly precipitation analysis (1979–present), *J. Hydrometeorol.*, *4*, 1147, doi:10.1175/1525-7541(2003)004<1147:TVGPCP>2.0.CO;2.
- Angell, J., and J. Korshover (1982), Comparison of year-average latitude, longitude and pressure of the four centers of action with air and sea temperature, 1899–1978, *Mon. Weather Rev.*, *110*, 300–303.
- Angell, J., and T. Korshover (1974), Quasi-biennial and long-term fluctuations in the centers of action, *Mon. Weather Rev.*, *102*, 669–678.
- Arimoto, R. (2001), Eolian dust and climate: Relationships to sources, tropospheric chemistry, transport and deposition, *Earth Sci. Rev.*, *54*, 29–42.
- Bakalian, F., S. Hameed, and R. Pickart (2007), Influence of the Icelandic Low latitude on the frequency of Greenland tip jet events: Implications for Irminger Sea convection, *J. Geophys. Res.*, *112*, C04020, doi:10.1029/2006JC003807.
- Baker, A., T. Jickells, M. Witt, and K. Linge (2006), Trends in the solubility of iron, aluminium, manganese and phosphorus in aerosol collected over the Atlantic Ocean, *Mar. Chem.*, *98*(1), 43–58, doi:10.1016/j.marchem.2005.06.004.
- Ben-Ami, Y., I. Koren, and O. Altartaz (2009), Patterns of North African dust transport over the Atlantic: Winter vs. summer, based on CALIPSO first year data, *Atmos. Chem. Phys.*, *9*, 7867–7875.
- Ben-Ami, Y., I. Koren, O. Altartaz, A. B. Kostinski, and Y. Lehahn (2011), Discernible rhythm in the spatio/temporal distributions of transatlantic dust, *Atmos. Chem. Phys. Discuss.*, *11*, 23,513–23,539, doi:10.5194/acpd-11-23513-2011.
- Carlson, T., and J. Prospero (1972), The large-scale movement of Saharan air outbreaks over the northern equatorial Atlantic, *J. Appl. Meteorol.*, *11*, 283–297.
- Chiapello, I., and C. Moulin (2002), TOMS and METEOSAT satellite records of the variability of Saharan dust transport over the Atlantic during the last two decades, *Geophys. Res. Lett.*, *29*(8), 1176, doi:10.1029/2001GL013767.
- Chiapello, I., G. Bergamietti, L. Gomes, B. Chatenet, F. Dulac, J. Pimenta, and E. Soares (1995), An additional low layer transport of Sahelian and Saharan dust over the north-eastern tropical Atlantic, *Geophys. Res. Lett.*, *22*, 3191–3194.
- Chiapello, I., J. Prospero, J. Herman, and N. Hsu (1999), Detection of mineral dust over the North Atlantic Ocean and Africa with the Nimbus 7 TOMS, *J. Geophys. Res.*, *104*, 9277–9291.
- Chiapello, I., C. Moulin, and J. M. Prospero (2005), Understanding the long-term variability of African dust transport across the Atlantic as recorded in both Barbados surface concentrations and large-scale Total Ozone Mapping Spectrometer (TOMS) optical thickness, *J. Geophys. Res.*, *110*, D18S10, doi:10.1029/2004JD005132.
- Christoforou, P., and S. Hameed (1997), Solar cycle and the Pacific 'centers of action,' *Geophys. Res. Lett.*, *24*, 293–296, doi:10.1029/97GL00017.
- Croke, M. S., R. D. Cess, and S. Hameed (1999), Regional cloud cover change associated with global climate change: Case studies for three regions of the United States, *J. Clim.*, *12*, 2128–2134, doi:10.1175/1520-0442(1999)012<2128:RCCCAW>2.0.CO;2.
- Darwin, C. (1846), An account of this fine dust which often falls on vessels in the Atlantic Ocean, *Q. J. Geol. Soc. London*, *2*, 26–30.
- DeMott, P. J., K. Sassen, M. R. Poellot, D. Baumgardner, D. C. Rogers, S. D. Brooks, A. J. Prenni, and S. M. Kreidenweis (2003), African dust aerosols as atmospheric ice nuclei, *Geophys. Res. Lett.*, *30*(14), 1732, doi:10.1029/2003GL017410.
- Doherty, O., N. Riemer, and S. Hameed (2008), Saharan mineral dust transport into the Caribbean: Observed atmospheric controls and trends, *J. Geophys. Res.*, *113*, D07211, doi:10.1029/2007JD009171.
- Dunion, J., and C. Velden (2004), The impact of the Saharan air layer on Atlantic tropical cyclone activity, *Bull. Am. Meteorol. Soc.*, *85*, 353–365.
- Engelstaedter, S., and R. Washington (2007), Atmospheric controls on the annual cycle of North African dust, *J. Geophys. Res.*, *112*, D03103, doi:10.1029/2006JD007195.
- Evans, A., J. Dunion, J. Foley, A. Heidinger, and C. Velden (2006a), New evidence for a relationship between Atlantic tropical cyclone activity and African dust outbreaks, *Geophys. Res. Lett.*, *33*, L19813, doi:10.1029/2006GL026408.
- Evans, A. T., A. K. Heidinger, and P. Knippertz (2006b), Analysis of winter dust activity off the coast of West Africa using a new 24-year over-water advanced very high resolution radiometer satellite dust climatology, *J. Geophys. Res.*, *111*, D12210, doi:10.1029/2005JD006336.
- Folland, C. K., T. N. Palmer, and D. E. Parker (1986), Sahel rainfall and worldwide sea temperatures, 1901–85, *Nature*, *320*, 602–607, doi:10.1038/320602a0.
- Folland, C., J. Owen, M. Ward, and A. Coleman (1991), Prediction of seasonal rainfall in the Sahel region using empirical and dynamical methods, *J. Forecast.*, *10*(1–2), 21–56.
- Formenti, P., et al. (2008), Regional variability of the composition of mineral dust from western Africa: Results from the AMMA SOP/DABEX and DODO field campaigns, *J. Geophys. Res.*, *113*, D00C13, doi:10.1029/2008JD009903.
- Giannini, A., R. Saravanan, and P. Chang (2003), Oceanic forcing of Sahel rainfall on interannual to interdecadal time scales, *Science*, *302*, 1027–1030, doi:10.1126/science.1089357.
- Ginoux, P., J. M. Prospero, O. Torres, and M. Chin (2004), Long-term simulation of global dust distribution with the GOCART model: Correlation with North Atlantic Oscillation, *Environ. Modell. Software*, *19*, 113–128.
- Glaccum, R. A., and J. M. Prospero (1980), Saharan aerosols over the tropical North Atlantic—Mineralogy, *Mar. Geol.*, *37*(3–4), 295–321, doi:10.1016/0025-3227(80)90107-3.
- Hameed, S., and S. Piontkovski (2004), The dominant influence of the Icelandic Low on the position of the Gulf Stream northwall, *Geophys. Res. Lett.*, *31*, L09303, doi:10.1029/2004GL019561.
- Herman, J., P. Bhartia, O. Torres, B. Holben, D. Tanre, T. Eck, A. Smirnov, B. Chatenet, and F. Lavenue (1997), Comparison of the TOMS aerosol index with Sun-photometer aerosol optical thickness: Results and applications, *J. Geophys. Res.*, *102*, 16,911–16,922.
- Herwitz, S., D. Muhs, J. Prospero, S. Mahan, and B. Vaughn (1996), Origin of Bermuda's clay-rich Quaternary paleosols and their paleoclimatic significance, *J. Geophys. Res.*, *101*, 23,389–23,400.
- Hoerling, M., J. Hurrell, J. Eischeid, and A. Phillips (2006), Detection and attribution of twentieth-century northern and southern African rainfall change, *J. Clim.*, *19*, 3989–4008, doi:10.1175/JCLI3842.1.
- Hurrell, J. (1995), Decadal trend in the North Atlantic Oscillation: Regional temperatures and precipitation, *Science*, *269*, 676–679.
- Jickells, T. (1999), The inputs of dust derived elements to the Sargasso sea: A synthesis, *Mar. Chem.*, *68*, 5–14.
- Jordi, A., and S. Hameed (2009), Influence of the Icelandic Low on the variability of surface air temperature in the Gulf of Lion: Implications for intermediate water formation, *J. Phys. Oceanogr.*, *39*, 3228, doi:10.1175/2009JPO4194.1.
- Kalnay, E., et al. (1996), The NCEP/NCAR 40-year reanalysis project, *Bull. Am. Meteorol. Soc.*, *77*, 437–471.
- Kapala, A., H. Mächel, and H. Flohn (1998), Behaviour of the centres of action above the Atlantic since 1881. Part II: Associations with regional climate anomalies, *Int. J. Climatol.*, *18*, 23–36.
- Kaufman, Y., I. Koren, L. Remer, D. Tanré, P. Ginoux, and S. Fan (2005), Dust transport and deposition observed from the Terra-Moderate Resolution Imaging Spectroradiometer (MODIS) spacecraft over the Atlantic Ocean, *J. Geophys. Res.*, *110*, D10S12, doi:10.1029/2003JD004436.
- Kiss, P., I. Janosi, and O. Torres (2007), Early calibration problems detected in TOMS Earth-Probe aerosol signal, *Geophys. Res. Lett.*, *34*, L07803, doi:10.1029/2006GL028108.
- Kolker, A. S., and S. Hameed (2007), Meteorologically driven trends in sea level rise, *Geophys. Res. Lett.*, *34*, L23616, doi:10.1029/2007GL031814.
- Koren, I., and Y. J. Kaufman (2004), Direct wind measurements of Saharan dust events from Terra and Aqua satellites, *Geophys. Res. Lett.*, *31*, L06122, doi:10.1029/2003GL019338.
- Lau, K. M., and K. M. Kim (2007), Cooling of the Atlantic by Saharan dust, *Geophys. Res. Lett.*, *34*, L23811, doi:10.1029/2007GL031538.
- Lau, K. M., K. M. Kim, Y. C. Sud, and G. K. Walker (2009), A GCM study of the response of the atmospheric water cycle of West Africa and the Atlantic to Saharan dust radiative forcing, *Ann. Geophys.*, *27*, 4023–4037, doi:10.5194/angeo-27-4023-2009.
- Lau, W. K. M., and K.-M. Kim (2007), How nature foiled the 2006 hurricane forecasts, *Eos Trans. AGU*, *88*, 105–106, doi:10.1029/2007EO090002.
- Levin, Z., A. Teller, E. Ganor, and Y. Yin (2005), On the interactions of mineral dust, sea-salt particles, and clouds: A measurement and modeling study from the Mediterranean Israeli Dust Experiment campaign, *J. Geophys. Res.*, *110*, D20202, doi:10.1029/2005JD005810.
- Mächel, H., A. Kapala, and H. Flohn (1998), Behaviour of the centres of action above the Atlantic since 1881. Part I: Characteristics of seasonal and interannual variability, *Int. J. Climatol.*, *18*, 1–22.

- Mahowald, N. M., and J.-L. Dufresne (2004), Sensitivity of TOMS aerosol index to boundary layer height: Implications for detection of mineral aerosol sources, *Geophys. Res. Lett.*, *31*, L03103, doi:10.1029/2003GL018865.
- Mahowald, N., C. Lou, J. del Corral, and C. Zender (2003), Interannual variability in atmospheric mineral aerosols from a 22-year model simulation and observational data, *J. Geophys. Res.*, *108*(D12), 4352, doi:10.1029/2002JD002821.
- Mohr, K. I., and C. D. Thorncroft (2006), Intense convective systems in West Africa and their relationship to the African easterly jet, *Q. J. R. Meteorol. Soc.*, *132*, 163–176, doi:10.1256/qj.05.55.
- Moulin, C., C. Lambert, F. Dulac, and U. Dayan (1997), Control of atmospheric export of dust from North Africa by the North Atlantic Oscillation, *Nature*, *387*, 691–694.
- Muhs, D. R., J. R. Budahn, J. M. Prospero, and S. N. Carey (2007), Geochronological evidence for African dust inputs to soils of western Atlantic islands: Barbados, the Bahamas, and Florida, *J. Geophys. Res.*, *112*, F02009, doi:10.1029/2005JF000445.
- Nicholson, S. E. (2009), A revised picture of the structure of the “monsoon” and land ITCZ over West Africa, *Clim. Dyn.*, *32*, 1155–1171, doi:10.1007/s00382-008-0514-3.
- Piontkovski, S., and S. Hameed (2002), Precursors of copepod abundance in the Gulf of Maine in atmospheric centers of action and sea surface temperature, *Global Atmos. Ocean Syst.*, *8*, 283–291.
- Prospero, J., and T. Carlson (1972), Vertical and areal distribution of Saharan dust over the western equatorial North Atlantic Ocean, *J. Geophys. Res.*, *77*, 5255–5265, doi:10.1029/JC077i027p05255.
- Prospero, J. M., and T. N. Carlson (1980), Saharan air outbreaks over the tropical North Atlantic, *Pure Appl. Geophys.*, *119*, 677–691, doi:10.1007/BF00878167.
- Prospero, J., and P. Lamb (2003), African droughts and dust transport to the Caribbean: Climate change implications, *Science*, *302*, 1024–1027.
- Prospero, J. M., and R. T. Nees (1977), Dust concentration in the atmosphere of the equatorial North Atlantic: Possible relationship to the Sahelian drought, *Science*, *196*, 1196–1198, doi:10.1126/science.196.4295.1196.
- Prospero, J., and R. Nees (1986), Impact of the North African drought and El Niño on mineral dust in the Barbados trade winds, *Nature*, *320*, 735–738.
- Prospero, J. M., E. Bonatti, C. Schubert, and T. N. Carlson (1970), Dust in the Caribbean atmosphere traced to an African dust storm, *Earth Planet. Sci. Lett.*, *9*, 287–293, doi:10.1016/0012-821X(70)90039-7.
- Prospero, J., P. Ginoux, O. Torres, S. Nicholson, and T. Gill (2002), Environmental characterization of global sources of atmospheric soil dust identified with the Nimbus 7 Total Ozone Mapping Spectrometer (TOMS) absorbing aerosol product, *Rev. Geophys.*, *40*(1), 1002, doi:10.1029/2000RG000095.
- Prospero, J. M., E. Blades, R. Naidu, G. Mathison, H. Thani, and M. C. Lavoie (2008), Relationship between African dust carried in the Atlantic trade winds and surges in pediatric asthma attendances in the Caribbean, *Int. J. Biometeorol.*, *52*, 823–832, doi:10.1007/s00484-008-0176-1.
- Riemer, N., O. Doherty, and S. Hameed (2006), On the variability of African dust transport across the Atlantic, *Geophys. Res. Lett.*, *33*, L13814, doi:10.1029/2006GL026163.
- Rosby, C.-G. (1939), Relation between variations in the intensity of the zonal circulation of the atmosphere and the displacement of the semi-permanent centers of actions, *J. Mar. Res.*, *2*, 38–55.
- Rydell, H. S., and J. M. Prospero (1972), Uranium and thorium concentrations in wind-borne Saharan dust over the Western Equatorial North Atlantic Ocean, *Earth Planet. Sci. Lett.*, *14*, 397–402, doi:10.1016/0012-821X(72)90140-9.
- Sankar-Rao, M., K. M. Lau, and S. Yang (1996), On the relationship between Eurasian snow cover and the Asian summer monsoon, *Int. J. Climatol.*, *16*, 605–616.
- Savoie, D. L., J. M. Prospero, and R. T. Nees (1987), Frequency distribution of dust concentration in Barbados as a function of averaging time, *Atmos. Environ.*, *21*(7), 1659–1663, doi:10.1016/0004-6981(87)90327-1.
- Schwanghart, W., and B. Schütt (2008), Meteorological causes of Harmattan dust in West Africa, *Geomorphology*, *95*, 412–428, doi:10.1016/j.geomorph.2007.07.002.
- Sokolik, I., and O. Toon (1996), Direct radiative forcing by anthropogenic airborne mineral aerosols, *Nature*, *381*, 681–683.
- Sultan, B., S. Janicot, and A. Diedhiou (2003), The West African Monsoon dynamics. Part I: Documentation of intraseasonal variability, *J. Clim.*, *16*, 3389–3406.
- Sunnu, A., G. Afeti, and F. Resch (2008), A long-term experimental study of the Saharan dust presence in West Africa, *Atmos. Res.*, *87*, 13–26.
- Swap, R., M. Garstang, S. Greco, R. Talbot, and P. Kallberg (1992), Saharan dust in the Amazon basin, *Tellus, Ser. B*, *44*, 133–149.
- Tegen, I., and I. Fung (1994), Modeling of mineral dust in the atmosphere: Sources, transport, and optical thickness, *J. Geophys. Res.*, *99*, 22,897–22,914, doi:10.1029/94JD01928.
- Tegen, I., A. Lacis, and I. Fung (1996), The influence of climate forcing of mineral aerosols from disturbed soils, *Nature*, *380*, 419–422.
- Tomas, R. A., J. R. Holton, and P. J. Webster (1999), The influence of cross-equatorial pressure gradients on the location of near-equatorial convection, *Q. J. R. Meteorol. Soc.*, *125*, 1107–1127, doi:10.1256/smsqj.55602.
- Torres, O., P. Bhartia, J. Herman, Z. Ahmad, and J. Gleason (1998), Derivation of aerosol properties from satellite measurements of back-scattered ultraviolet radiation: Theoretical basis, *J. Geophys. Res.*, *103*, 17,099–17,110.
- Torres, O., P. Bhartia, J. Herman, A. Sinyuk, P. Ginoux, and B. Holben (2002), A long-term record of aerosol optical depth from TOMS observations and comparison to AERONET measurements, *J. Atmos. Sci.*, *59*, 398–413.
- Trapp, J. M., F. J. Millero, and J. M. Prospero (2010), Temporal variability of the elemental composition of African dust measured in trade wind aerosols at Barbados and Miami, *Mar. Chem.*, *120*(1–4), 71–82, doi:10.1016/j.marchem.2008.10.004.
- Walsh, J. J., and K. A. Steidinger (2001), Saharan dust and Florida red tides: The cyanophyte connection, *J. Geophys. Res.*, *106*, 11,597–11,612, doi:10.1029/1999JC000123.
- Washington, R., and M. Todd (2005), Atmospheric controls on mineral dust emission from the Bodele Depression, Chad: The role of the low level jet, *Geophys. Res. Lett.*, *32*, L17701, doi:10.1029/2005GL023597.
- Washington, R., M. Todd, and A. G. N. Middleton (2003), Dust-storm source areas determined by the Total Ozone Monitoring Spectrometer and surface observations, *Ann. Assoc. Am. Geogr.*, *93*, 297–313.
- Wilcox, E. M., K. M. Lau, and K.-M. Kim (2010), A northward shift of the North Atlantic Ocean Intertropical Convergence Zone in response to summertime Saharan dust outbreaks, *Geophys. Res. Lett.*, *37*, L04804, doi:10.1029/2009GL041774.
- Wilks, D. (1995), *Statistical Methods in the Atmospheric Sciences: An Introduction*, Academic, San Diego, Calif.
- Zender, C. S., H. Bian, and D. Newman (2003), Mineral Dust Entrainment and Deposition (DEAD) model: Description and 1990s dust climatology, *J. Geophys. Res.*, *108*(D14), 4416, doi:10.1029/2002JD002775.